Decipher the sensitivity of urban canopy air temperature to anthropogenic heat flux with a forcing-feedback framework

Linying Wang[a*], Ting Sun[b], Wenyu Zhou[c], Maofeng Liu[d], Dan Li[a]

[a] *Department of Earth and Environment, Boston University, Boston, Massachusetts*

[b] *Institute for Risk and Disaster Reduction, University of College London, London, United Kingdom*

[c] *Atmospheric Sciences & Global Change, Pacific Northwest National Laboratory, Richland, Washington*

[d] *Rosenstiel School of Marine, Atmospheric, and Earth Science, University of Miami, Miami, Florida*

* *Corresponding author*: Linying Wang, wangly@bu.edu

ABSTRACT

The sensitivity of urban canopy air temperature (T_a) to anthropogenic heat flux (Q_{AH}) is known to vary with space and time, but the key factors controlling such spatiotemporal variabilities remain elusive. To quantify the contributions of different physical processes to the magnitude and variability of $\Delta T_a/\Delta Q_{AH}$ (where Δ represents a change), we develop a forcing-feedback framework based on the energy budget of air within the urban canopy layer and apply it to diagnosing $\Delta T_a/\Delta Q_{AH}$ simulated by the Community Land Model Urban (CLMU) over the contiguous United States (CONUS). In summer, the median $\Delta T_a/\Delta Q_{AH}$ is around 0.01 $K\ (W\ m^{-2})^{-1}$ over CONUS. Besides the direct effect of Q_{AH} on T_a, there are important feedbacks through changes in the surface temperature, the atmosphere-canopy air heat conductance (c_a), and the surface-canopy air heat conductance. The positive and negative feedbacks nearly cancel each other and $\Delta T_a/\Delta Q_{AH}$ is mostly controlled by the direct effect in summer. In winter, $\Delta T_a/\Delta Q_{AH}$ becomes stronger, with the median value increased by about 20% due to weakened negative feedback associated with c_a. The spatial and temporal (both seasonal and diurnal) variability of $\Delta T_a/\Delta Q_{AH}$ as well as the nonlinear response of ΔT_a to ΔQ_{AH} are strongly related to the variability of c_a, highlighting the importance of correctly parameterizing convective heat transfer in urban canopy models.

Keywords: climate sensitivity, urban canopy layer, anthropogenic heat flux, forcing-feedback framework, land surface model

1. Introduction

Anthropogenic heating resulting from energy consumption by human activities is an important control of urban climate. Although occupying only 3% of Earth's surface, cities consume 60-80% of global energy and house more than half of the human population (United Nations 2022). The intense anthropogenic heating in cities can increase heat stress (Doan et al. 2019; Jin *et al* 2020; Molnár *et al* 2020), which threatens thermal comfort and causes heat-related illnesses (Mora *et al* 2017). Studies have found that a 1 ℃ air warming is associated with an increase in mortality rate by 1.8% in cities when the daily temperature is higher than 28 ℃ (Chan *et al* 2012). Meanwhile, a higher temperature resulting from anthropogenic heating also affects cooling energy demand, air quality, ecosystems, and so on (Fink *et al* 2014; Liu *et al* 2020; Salamanca *et al* 2014; Xie *et al* 2016). Furthermore, anthropogenic heat flux affects meteorological processes within the urban boundary layer (Bohnenstengel *et al* 2014; Chen *et al* 2009; Fan and Sailor 2005; Krpo *et al* 2010; Ma *et al* 2017; Mei and Yuan 2021; Molnár *et al* 2020; Suga *et al.* 2009; Zhang *et al* 2016).

Anthropogenic heat flux is generated from many sources, including building and industrial energy consumption, traffic, and human metabolism (Chow *et al* 2014; Sailor 2011; Sun *et al* 2018). The magnitude of anthropogenic heat flux varies strongly with the local climate, population density, economy, and technology (Allen *et al* 2011; Fan and Sailor 2005; Jin *et al* 2020; Sailor *et al* 2015; Yang *et al* 2017). The magnitude of anthropogenic heat flux is also scale dependent. At long-term and city (or larger) scales, the anthropogenic heat flux is typically on the order of 0.1-1 $\mathrm{W\ m^{-2}}$. For example, Sailor *et al* (2015) developed a national database of anthropogenic heat flux over the contiguous United States (CONUS) and showed that the maximum wintertime (summertime) anthropogenic heat flux is around 0.8-0.97 $\mathrm{W\ m^{-2}}$ (0.47-0.63 $\mathrm{W\ m^{-2}}$) across 61 U.S. cities. Another study reported that the annual-mean anthropogenic heat flux is around 0.39

57 $W\ m^{-2}$, 0.68 $W\ m^{-2}$ and 0.22 $W\ m^{-2}$ for COUNS, western Europe, and China, respectively, and
58 only 0.028 W m^{-2} on the global scale (Flanner 2009). However, the short-term and neighborhood-
59 scale anthropogenic heat flux can be much stronger (Sailor and Lu 2004). Ichinose *et al* (1999)
60 showed that the anthropogenic heat flux in central Tokyo exceeded 400 $W\ m^{-2}$ in the daytime,
61 and the maximum value reached 1590 $W\ m^{-2}$ in the early morning of winter.

62 Previous studies on the effects of anthropogenic heat flux on urban climate were typically
63 conducted using weather and climate models. Salamanca *et al* (2014) quantified the impacts of
64 anthropogenic heat flux via turning on/off air conditioning systems in the Weather Research and
65 Forecasting (WRF) model coupled to a building energy model (BEM) and a multilayer building
66 effect parameterization (BEP). Their results revealed that the heat emitted from air conditioning
67 systems resulted in a 1-1.5 ℃ temperature rise during summer nights over Phoenix (U.S.). Fan and
68 Sailor (2005) incorporated an anthropogenic heating source term in the near-surface energy
69 balance within the NCAR/PennState Fifth Generation Model (MM5). They found that the
70 influence of anthropogenic heat flux on the urban climate of Philadelphia (U.S.) was significant,
71 particularly during nighttime and in winter, with the near-surface air warming as large as 2-3 ℃.
72 Similar results were also found in China (Feng *et al* 2012; Feng *et al* 2014) and Australia (Ma *et*
73 *al* 2017), where the temperature rise was more pronounced in winter than summer. In another
74 numerical study conducted in a Japanese megacity (Keihanshin district), the results indicated that
75 although the daytime anthropogenic heat flux was larger than the nighttime counterpart, the
76 induced temperature rise was nearly threefold larger at night (Narumi *et al* 2009). Studies also
77 revealed that the anthropogenic heating effects depended on not only the quantity of anthropogenic
78 heat flux, but also atmospheric stratification as well as orographic factors (Block *et al* 2004;
79 Narumi *et al* 2009; Zhang *et al* 2016).

Since it is obvious that the amount of warming induced by anthropogenic heating depends on the magnitude of anthropogenic heat flux, it is perhaps more important to examine the ratio of the temperature increase to the amount of anthropogenic heat flux ($\Delta T_a/\Delta Q_{AH}$, where Δ represents a change), much like the concept of climate sensitivity but at the local (urban) scale. In this sense, we treat the change in anthropogenic heat flux (ΔQ_{AH}) as the climate *forcing* and the change in urban temperature (ΔT_a) as the climate *response*. Table 1 provides a selected list of existing studies on the warming effect of anthropogenic heat flux. By normalizing the temperature increase by the magnitude of anthropogenic heat flux, a better consistency among different studies emerges, with the magnitude of $\Delta T_a/\Delta Q_{AH}$ on the order of 0.01 $K(W\ m^{-2})^{-1}$. This value is consistent with the findings in Kikegawa *et al* (2014), who carried out field campaigns based on meteorological measurements and electricity demand monitoring, as well as numerical simulations with WRF (coupled with a multilayer urban canopy model and a building energy model) in two Japanese major cities, Tokyo and Osaka, in July to August 2007. Their work suggested an afternoon sensitivity of 0.01 $K\ (W\ m^{-2})^{-1}$ based on observations and showed that the simulated results had the same order of magnitude. However, it is noteworthy to point out that the magnitude of $\Delta T_a/\Delta Q_{AH}$ from different studies (table 1) still varies by nearly two orders of magnitude (from 0.001 to 0.05 $K\ (W\ m^{-2})^{-1}$). More importantly, the physical processes responsible for such variability remain elusive. Quantifying the key factors controlling the variability of $\Delta T_a/\Delta Q_{AH}$ frames the scope of this study.

To do so, we develop a forcing-feedback framework based on the energy budget of air within the urban canopy layer and apply it to diagnosing $\Delta T_a/\Delta Q_{AH}$ simulated by the Community Land Model Urban (CLMU) over CONUS, which has a growing urban population and consumes considerable energy in cities. The impact of anthropogenic heat over the entire CONUS has not

been investigated. This study is organized as follows: Section 2 describes the forcing-feedback framework and model experiments. Section 3 evaluates $\Delta T_a/\Delta Q_{AH}$ at the seasonal and diurnal scales. The key feedback mechanisms and the factors controlling the variability of $\Delta T_a/\Delta Q_{AH}$ are discussed in detail in this section. Finally, discussions and conclusions are presented in Section 4 and Section 5, respectively.

2. Methodology

2.1. A forcing-feedback framework

We propose a forcing-feedback framework to diagnose the sensitivity of air temperature within the urban canopy layer (UCL, i.e., the layer below the height of the main urban elements), also called urban canopy air temperature hereafter, to anthropogenic heat flux based on the energy budget of air within the UCL (figure 1). This conceptualization of the UCL is consistent with the theoretical underpinning of nearly all single-layer urban canopy models (UCMs) in weather and climate modeling, including the Community Land Model - Urban (CLMU) to be used in this study (more details on CLMU are presented later). Our starting point is that the UCL is our control volume (or system of interest) and is the direct recipient of anthropogenic heat flux (i.e., the forcing). At steady state, the energy budget of the air within UCL can be written as

$$0 = Q_{AH} + R \tag{1}$$

where Q_{AH} is the anthropogenic heat flux and R is the sum of heat fluxes other than the anthropogenic heat flux (more about R later). When the anthropogenic heat flux is altered by a certain amount (indicated by Δ), the energy balance of air within the UCL reaches a new equilibrium state,

$$0 = \Delta Q_{AH} + \Delta R \tag{2}$$

where ΔQ_{AH} can be interpreted as the added anthropogenic heat flux compared to the scenario without anthropogenic heat flux, and ΔR is the total change of other heat fluxes in response to ΔQ_{AH}.

Changes in other heat fluxes (ΔR) are often related to changes in the canopy air temperature (ΔT_a). Denoting $\Delta R = \lambda_{all}\Delta T_a$, we can write the sensitivity of canopy air temperature to anthropogenic heat flux as

$$\frac{\Delta T_a}{\Delta Q_{AH}} = -\frac{1}{\lambda_{all}} \tag{3}$$

where λ_{all} is the sensitivity parameter (called the total sensitivity parameter in order to distinguish it from other feedback parameters introduced later). The sensitivity $\Delta T_a/Q_{AH}$, which indicates how easily the canopy air temperature can be altered by a perturbation of anthropogenic heat flux, is thus equivalent to the negative reciprocal of the total sensitivity parameter (λ_{all}). If the absolute value of λ_{all} is larger, the canopy air warming per unit increase of anthropogenic heat flux is weaker. Therefore, to understand the sensitivity $\Delta T_a/Q_{AH}$, we need to examine the total sensitivity parameter (λ_{all}) in the relation $\Delta R = \lambda_{all}\Delta T_a$.

The air within the UCL receives convective heat fluxes from various urban surfaces and the overlying atmosphere. The sum of these heat fluxes (R) received by the air within the UCL can thus be written as

$$R = \sum_{i=1}^{n} \rho C_p w_i c_s \left(T_s^i - T_a\right) + \rho C_p c_a (\theta_{atm} - T_a) \tag{4}$$

where n is the number of urban surfaces (e.g., there are five urban surfaces in CLMU that interact with the canopy air, including roof, previous ground, imperious ground, sun wall, and shade wall), i refers to the i^{th} urban surface, w_i is the weight of the i^{th} surface based on the corresponding area fraction (converted to per unit area of urban canyon floor in the horizontal direction), ρ is the air density (kg m^{-3}), C_p is the specific heat of air at constant pressure assumed to be of a constant value of 1004.64 J kg^{-1} K^{-1}, c_s is the heat conductance between the air within the UCL and the urban

surface (called the surface-canopy air heat conductance, m s^{-1}), c_a is the heat conductance between the air within the UCL and the overlying atmosphere (called the atmosphere-canopy air heat conductance, m s^{-1}), T_s is the urban surface temperature (K), and θ_{atm} is the atmospheric potential temperature (K). Here we have assumed that the heat conductances between the air within the UCL and different urban surfaces are identical, which is a common assumption made in CLMU and many other single-layer UCMs. But this assumption can be relaxed by allowing c_s to vary for different urban surfaces in future work.

With equation (4), the total sensitivity parameter λ_{all} can be written as the sum of the direct effect and feedbacks. Using the chain rule on equation (4) yields

$$\lambda_{all} = \frac{\Delta R}{\Delta T_a} = \frac{\partial R}{\partial T_a} + \sum_{i=1}^{n} \frac{\partial R}{\partial T_s^i}\frac{\Delta T_s^i}{\Delta T_a} + \frac{\partial R}{\partial c_a}\frac{\Delta c_a}{\Delta T_a} + \frac{\partial R}{\partial c_s}\frac{\Delta c_s}{\Delta T_a} + \frac{\partial R}{\partial \theta_{atm}}\frac{\Delta \theta_{atm}}{\Delta T_a} \quad (5)$$
$$= \lambda_0 + \lambda_1 + \lambda_2 + \lambda_3 + \lambda_4$$

where the partial and total derivatives are denoted by ∂ and Δ, respectively. In this equation, λ_0 is the baseline sensitivity parameter, representing the direct effect of anthropogenic heat flux on canopy air temperature with everything else (e.g., surface temperature, atmosphere-canopy air heat conductance, etc) held the same. Other λ parameters represent different feedback processes: λ_1 refers to the strength of feedback from changes in surface temperatures; λ_2 is the feedback parameter for changes in atmosphere-canopy air heat conductance; λ_3 is the feedback parameter for changes in surface-canopy air heat conductance; and λ_4 is the parameter for atmospheric feedback. A positive (or negative) feedback means that the process leads to an amplification (or dampening) of the direct effect of anthropogenic heat flux on canopy air temperature.

Combining equation (4) and (5), the baseline sensitivity parameter and feedback parameters can be derived as

$$\lambda_0 = \frac{\partial R}{\partial T_a} = -\rho C_p \left(\sum_{i=1}^{n} w_i c_s + c_a \right) \tag{6}$$

$$\lambda_1 = \sum_{i=1}^{n} \frac{\partial R}{\partial T_s^i} \frac{\Delta T_s^i}{\Delta T_a} = \sum_{i=1}^{n} \rho C_p w_i c_s \frac{\Delta T_s^i}{\Delta T_a} \tag{7}$$

$$\lambda_2 = \frac{\partial R}{\partial c_a} \frac{\Delta c_a}{\Delta T_a} = \rho C_p (\theta_{atm} - T_a) \frac{\Delta c_a}{\Delta T_a} \tag{8}$$

$$\lambda_3 = \frac{\partial R}{\partial c_s} \frac{\Delta c_s}{\Delta T_a} = \left(\sum_{i=1}^{n} \rho C_p w_i \left(T_s^i - T_a \right) \right) \frac{\Delta c_s}{\Delta T_a} \tag{9}$$

$$\lambda_4 = \frac{\partial R}{\partial \theta_{atm}} \frac{\Delta \theta_{atm}}{\Delta T_a} = \rho C_p c_a \frac{\Delta \theta_{atm}}{\Delta T_a} \tag{10}$$

Equation (1) to (10) constitute our forcing-feedback framework for diagnosing the sensitivity of canopy air temperature to anthropogenic heat flux. The aim of the proposed forcing-feedback framework is not to predict $\Delta T_a / \Delta Q_{AH}$, but to provide a diagnostic tool for quantifying the strengths of direct effects and feedback processes. In this study, the inputs for this framework are the simulated results from CLMU. However, this framework is not limited to CLMU and can be applied to diagnosing outputs from other UCMs.

2.2. The CLMU model and the numerical experiment design

CLMU is the urban parameterization within the Community Land Model (CLM), which is the land component of the Community Earth System Model (CESM) (Danabasoglu *et al* 2020). In this study, the most recent released version of CLM (CLM5) within the framework of CESM version 2 (CESM2) is used. Within each land grid cell, CLM5 can have multiple land units including

vegetated, crop, urban, glacier, and lakes. For each urban land unit, three urban categories (tall building district, high density, and medium density) are allowed. In CLMU, the urban canyon system consists of five surfaces: roofs, sunlit and shaded walls, impervious and pervious floors. The energy and water fluxes from each urban surface interact with the canopy air (see figure 1). A more detailed description of CLMU including the main urban parameters can be found elsewhere (Oleson *et al.* 2010; Oleson and Feddema 2020). The CLMU input data are supplied by a global dataset (Jackson *et al.* 2010). The model has been widely used to study urban energy and water fluxes, as well as surface and air temperatures (Demuzere *et al* 2013; Grimmond *et al* 2011; Karsisto *et al* 2016; Oleson *et al* 2008a; Oleson *et al* 2008b; Oleson and Feddema 2020). In this study, we use an improved CLMU that includes parameterizations of urban heat mitigation strategies (e.g., cool roofs and green roofs), which have been proposed and validated in our previous work (Wang *et al* 2020, 2021), although these new features are not used in this study.

We run CLM5 in an offline mode (i.e., forced by meteorological data) at a 1/8 degree spatial resolution over CONUS and at an hourly time step. The hourly meteorological forcing data is from the North America Land Data Assimilation System phase II (NLDAS2) dataset (Xia *et al* 2012). The model is first spin up for 84 years by recycling the 1979-1999 NLDAS2 forcing four times. Four sets of numerical experiments are then conducted from 1979 to 1999 using the same initial condition obtained from the spin up run (table S1). These four numerical experiments are designed to quantify how the canopy air temperature (figure 1) responds to a prescribed increase of anthropogenic heat flux. In the control (CTL) experiment, no anthropogenic heat flux is added to the urban canopy air heat budget, and the simulated canopy air temperature is denoted as $T_{a,0}$. In the first sensitivity experiment (AH1), we add 1 W m^{-2} of anthropogenic heat flux into the urban canopy air heat budget at each time step and compute a new canopy air temperature (hereafter

199 $T_{a,1}$). Therefore, the difference between $T_{a,1}$ and $T_{a,0}$ (which is numerically equivalent to
200 $\Delta T_a/\Delta Q_{AH}$ given that the added anthropogenic heat flux is 1 W m^{-2}) is the total impact of 1
201 W m^{-2} of anthropogenic heat flux, which includes both the direct effect and the feedbacks. In
202 another two sensitivity experiments AH10 and AH100, the added anthropogenic heat flux is 10
203 W m^{-2} and 100 W m^{-2}, respectively. We denote the simulated canopy air temperatures in these
204 two experiments as $T_{a,10}$ and $T_{a,100}$, respectively. The sensitivity $\Delta T_a/\Delta Q_{AH}$ is thus calculated as
205 $(T_{a,10} - T_{a,0})/10$ and $(T_{a,100} - T_{a,0})/100$, respectively (see table S1). These two sensitivity
206 experiments (AH10 and AH100) are designed to quantify whether the sensitivity $\Delta T_a/\Delta Q_{AH}$ is
207 influenced by the magnitude of anthropogenic heat flux due to nonlinearity in the feedback
208 processes. We choose these values (1, 10, 100 W m^{-2}) to cover a wide but reasonable range of
209 anthropogenic heat flux magnitude.

210 We should emphasize that the added anthropogenic heat flux in all our experiments is
211 prescribed, not computed by the building energy model in CLMU (Demuzere *et al* 2013; Oleson
212 *et al* 2011). We prescribe the added anthropogenic heat flux because we are mostly interested in
213 the sensitivity of canopy air temperature to anthropogenic heat flux, not what processes generate
214 the anthropogenic heat flux. Moreover, when the building energy model in CLMU is used, the
215 generated anthropogenic heat flux is added to the pervious and impervious surface energy budgets,
216 which seems unphysical and is avoided in our study. Another way of interpreting our results is that
217 they represent the sensitivity of urban canopy air temperature to anthropogenic heat fluxes from
218 non-building (e.g., transportation) sectors with the magnitude of 1, 10, and 100 W m^{-2}.

219 For all simulations, we output the hourly urban canopy air temperatures, the temperatures of
220 different urban surfaces (i.e., roof, walls, and canyon floors), the surface-canopy air heat
221 conductance (c_s), as well as the atmosphere-canopy air heat conductance (c_a). Note that the

outputted c_s and c_a are computed internally via their parameterizations in CLMU. These hourly outputs are then used in the forcing-feedback framework described in Section 2.1. Specifically, we compute the hourly sensitivity parameters based on equations (6) - (9). Given that we do not have atmospheric feedbacks in our simulations, $\lambda_4 = 0$. With the sensitivity parameters calculated using equations (6) - (9), the total sensitivity ($\Delta T_a/\Delta Q_{AH}$) can be diagnosed using equations (3) and (5). The diagnosed $\Delta T_a/\Delta Q_{AH}$ is then compared to the directly computed $\Delta T_a/\Delta Q_{AH}$ mentioned above (e.g., for AH1 the directly computed $\Delta T_a/\Delta Q_{AH}$ is simply $T_{a,1} - T_{a,0}$). We average the hourly results over 20 years from 1980 to 1999.

Before we move to the results section, it is informative to briefly discuss the physics behind c_a and c_s and their parameterizations in CLMU, as they are key parameters in the forcing-feedback framework (see e.g., equation (6)). Physically, c_a (c_s) represents the efficiency of convective heat transfer between the overlying atmosphere (the urban surfaces) and the canopy air. Given that the flow within the UCL is turbulent, both c_a and c_s are strongly affected by shear and buoyancy, the two main sources of turbulence kinetic energy. However, c_a and c_s are fundamentally different because they represent the convective heat transfer efficiencies across different levels. In terms of their parameterizations in CLMU, c_a is parameterized through the classic Monin-Obukhov similarity theory (Oleson *et al* 2008a). Hence, c_a is strongly affected by atmospheric stratification. However, c_s is parameterized as only a function of wind speed in the urban canyon (Oleson *et al* 2008a) and is thus much less affected by atmospheric stratification compared to c_a.

3. Results

3.1. Sensitivity of canopy air temperature to anthropogenic heat flux ($\Delta T_a/\Delta Q_{AH}$) and the associated feedback parameters

We first present the sensitivity $\Delta T_a/\Delta Q_{AH}$ simulated by CLMU in summer (June-August, or JJA) and winter (December-February, or DJF) seasons (figure 2). The results shown here have been averaged over 20 years (1980-1999) and are based on the AH1 experiment where the added anthropogenic heat flux is 1 $W\ m^{-2}$. The effect of increasing the magnitude of anthropogenic heat flux will be discussed in Section 3.4. In summer, the median value of the sensitivity $\Delta T_a/\Delta Q_{AH}$ is around 0.01 $K\ (W\ m^{-2})^{-1}$, broadly comparable with previous studies presented in table 1. Here the median values are shown to minimize the influence of outliers. In winter, the sensitivity $\Delta T_a/\Delta Q_{AH}$ becomes stronger, with the median value increased by about 20%. In some cities in the southwestern U.S. (e.g., Los Angeles and Phoenix), the winter values of $\Delta T_a/\Delta Q_{AH}$ even reach 0.03 $K\ (W\ m^{-2})^{-1}$.

To understand the directly computed $\Delta T_a/\Delta Q_{AH}$ from CLMU simulation results, we employ the forcing-feedback framework described in Section 2.1. The total sensitivity diagnosed from this framework (i.e., using equations (5) - (9)) matches very well with the directly computed $\Delta T_a/\Delta Q_{AH}$ (figure 2), with spatial correlation coefficients larger than 0.99. These results give us confidence to use the forcing-feedback framework to interpret $\Delta T_a/\Delta Q_{AH}$.

Based on the forcing-feedback framework, the total sensitivity parameter (λ_{all}) can be decomposed into the sum of the baseline sensitivity parameter (λ_0) and the feedback parameters (λ_1, λ_2, and λ_3). We find that the magnitude of λ_{all} is almost identical to the magnitude of λ_0 (the spatial median value is -122 $W\ m^{-2}\ K^{-1}$ for both λ_{all} and λ_0) in summer (figure 3). This is because the sum of the three feedback parameters ($\lambda_1 + \lambda_2 + \lambda_3$) is very small, with the positive feedbacks and negative feedbacks nearly cancelling each other. The positive feedback is mainly from changes in surface temperatures (λ_1, with a median value of 24 $W\ m^{-2}\ K^{-1}$). This is expected as increases in surface temperature due to the added anthropogenic heat flux can in turn

amplify the canopy air warming. On the other hand, the negative feedback is mainly the result of changes in atmosphere-canopy air heat conductance (λ_2, with a median value of -25 $W\ m^{-2}\ K^{-1}$). As the anthropogenic heat flux is added, the atmospheric stratification is altered (i.e., relatively more unstable), resulting in increased atmosphere-canopy air heat conductance (c_a). This in turn leads to an increase in heat transfer into the overlying atmosphere and a dampening of the canopy air warming signal. The feedback from changes in surface-canopy air heat conductance (λ_3, with a median value of 1 $W\ m^{-2}\ K^{-1}$) is much weaker than the other two feedback processes. This can be explained by the parameterization of surface-canopy air heat conductance (c_s) in CLMU, which is only dependent on the wind speed in the UCL and thus is a much weaker function of atmospheric stratification than the atmosphere-canopy air heat conductance (c_a).

In winter (figure 3), the negative feedback from atmosphere-canopy air heat conductance (λ_2) decreases in its magnitude by 11 $W\ m^{-2}\ K^{-1}$ (in terms of median value) when compared to its summer counterpart (see also figure S1 for a comparison between summer and winter results). Namely, λ_2 becomes less negative, implying that the negative feedback from atmosphere-canopy air heat conductance (c_a) is weakened. Unlike the reduced magnitude of λ_2 in winter, the winter-summer differences in λ_1 and λ_3 are much smaller (about 1 $W\ m^{-2}\ K^{-1}$ in terms of median values) and almost negligible. As a result, the sum of feedbacks ($\lambda_1 + \lambda_2 + \lambda_3$) becomes positive in winter (compared to nearly zero in summer). The absolute value of the total sensitivity parameter (λ_{all}) therefore decreases, which further leads to an increase in the sensitivity $\Delta T_a/\Delta Q_{AH}$. The weakened negative feedback from atmosphere-canopy air heat conductance (c_a) explains why stronger canopy air warming is observed in winter than in summer with the same amount of anthropogenic heat flux (figure 2), a typical result in the literature.

3.2. Spatial variability of the sensitivity ($\Delta T_a/\Delta Q_{AH}$) and its controlling factors

Figure 2 exhibits strong spatial variabilities in the sensitivity $\Delta T_a/\Delta Q_{AH}$. To understand these spatial variabilities, we first note that the spatial pattern of the baseline sensitivity parameter λ_0 is very close to that of λ_{all}, with spatial correlation coefficients of 0.77 and 0.95 in summer and winter, respectively. Therefore, the spatial variability of λ_0 largely determines the spatial variability of the sensitivity $\Delta T_a/\Delta Q_{AH}$. From equation (6), λ_0 is proportional to the sum of atmosphere-canopy air heat conductance (c_a) and surface-canopy air heat conductance (c_s). We find that c_s is less than 20% of c_a and shows little spatial variability (not shown). As a result, one would expect that the spatial variability of λ_0 is mainly controlled by the spatial variability of c_a.

This is indeed the case. We find that the spatial correlation coefficients between λ_0 and c_a are very strong (-0.87 and -0.98 in summer and winter, respectively). The negative correlations are understandable since physically the atmosphere-canopy air heat conductance (c_a) indicates how strongly the air within the UCL communicates with the overlying atmosphere in terms of convective heat transfer. In places with larger (smaller) c_a, it is easier (more difficult) to transfer heat from the UCL to the overlying atmosphere, and thus the canopy air warming signal is weaker (stronger) with the same amount of anthropogenic heat flux.

3.3. Diurnal variation of the sensitivity ($\Delta T_a/\Delta Q_{AH}$) and its controlling factors

We further analyze the diurnal variation of $\Delta T_a/\Delta Q_{AH}$. To do so, we select four metropolitan cities that have widely different climates and geographical locations (San Francisco, Boston, Chicago, and Houston), instead of presenting averaged results over the CONUS.

In summer (figure 4(a)), all four cities experience a higher $\Delta T_a/\Delta Q_{AH}$ in the early morning than in other times. The morning peak of $\Delta T_a/\Delta AH$ is around 0.038 $K\ (W\ m^{-2})^{-1}$ in Houston, followed by San Francisco, Boston, and Chicago. In the afternoon, the sensitivity in all cities is

close to 0.01 $K\ (W\ m^{-2})^{-1}$, which is consistent with the findings of Kikegawa *et al* (2014) that also suggested a summer afternoon sensitivity of 0.01 $K\ (W\ m^{-2})^{-1}$. In contrast, there exist large differences in the diurnal variation of $\Delta T_a/\Delta Q_{AH}$ in winter (figure 4(b)). The sensitivity $\Delta T_a/\Delta Q_{AH}$ in Boston and Chicago is around 0.01 $K\ (W\ m^{-2})^{-1}$ throughout the day with small diurnal variations, while the diurnal variations of $\Delta T_a/\Delta Q_{AH}$ in Houston and San Francisco are strong, with much larger nighttime values than daytime values. San Francisco has the largest sensitivity in winter among the four cities with a peak value of 0.036 $K\ (W\ m^{-2})^{-1}$.

According to the forcing-feedback framework, the diurnal variations of $\Delta T_a/\Delta Q_{AH}$ are linked to the diurnal variations of feedback parameters, including the baseline sensitivity parameter (λ_0). As shown in figure 4(c-l), λ_0 and, to a lesser extent, λ_2 exhibit diurnal variations that resemble those of λ_{all}, implying that the diurnal variations of $\Delta T_a/\Delta Q_{AH}$ are controlled by processes encoded in λ_0 (equation (6)) and, to a lesser extent, λ_2 (equation (8)). Close inspection of equations (6) and (8) indicates that a common process in equations (6) and (8) is the atmosphere-canopy air heat conductance (c_a), suggesting that the diurnal variation of c_a (and Δc_a) are the key to understanding the diurnal variation of $\Delta T_a/\Delta Q_{AH}$.

The atmosphere-canopy air heat conductance (c_a) is controlled by shear- and buoyancy-generated turbulence and thus is strongly affected by atmospheric stratification. In winter, the air within UCL experiences more stable conditions at night, and hence c_a is smaller, λ_0 is less negative (figure 4(f)), and $\Delta T_a/\Delta Q_{AH}$ is larger (figure 4(b)) than their daytime counterparts, assuming that the shear is the same between daytime and nighttime. In summer, the accumulation of stable stratification throughout the night reduces c_a (leading to less negative λ_0, figure 4(e)) and increases $\Delta T_a/\Delta Q_{AH}$ (figure 4(a)). After sunrise, the stratification transitions from stable to unstable, which increases c_a, causes more negative λ_0, and reduces $\Delta T_a/\Delta Q_{AH}$. These two

processes yield a morning peak of $\Delta T_a/\Delta Q_{AH}$, as observed in figure 4(a). Shear also plays an important role. For example, the stronger winds in Boston and Chicago in winter likely cause larger shear, leading to larger c_a and smaller $\Delta T_a/\Delta Q_{AH}$, when compared to Houston and San Francisco (figure 4(b)).

3.4. Nonlinear response of ΔT_a to ΔQ_{AH}

The above results are from the AH1 experiment, which adds 1 $W\ m^{-2}$ of anthropogenic heat flux into the UCL. We also conduct experiments to investigate how the canopy air temperature responds to different amounts of anthropogenic heat flux. The aim of these experiments is to test whether any of the feedbacks scale nonlinearly with ΔQ_{AH}, thereby creating nonlinear responses of ΔT_a to ΔQ_{AH}. Note that the baseline sensitivity parameter (λ_0, see equation (6)) does not change with the magnitude of anthropogenic heat flux. Thus, any nonlinear response must stem from the feedback processes.

Figure 5 presents the relative changes in the sensitivity ($\Delta T_a/\Delta Q_{AH}$) and feedback parameters (λ_1, λ_2, λ_3) by comparing AH10 and AH100 to AH1 (i.e., the results of AH10 and AH100 minus the results of AH1 and then normalized by the results of AH1). The relative changes in the sensitivity ($\Delta T_a/\Delta Q_{AH}$) are all negative, implying that the sensitivity becomes smaller as the magnitude of anthropogenic heat flux increases. The relative changes between AH100 and AH1 in terms of the sensitivity $\Delta T_a/\Delta Q_{AH}$ have median values of -27% and -35% in summer and winter, respectively. This suggests that ΔT_a does respond nonlinearly to ΔQ_{AH}. Here we should stress that this result does not mean that changes in canopy air temperature ΔT_a become smaller as the magnitude of anthropogenic heat flux increases. It is rather the sensitivity ($\Delta T_a/\Delta Q_{AH}$) that reduces as the magnitude of anthropogenic heat flux increases.

The relative changes in feedback parameters suggest that the nonlinear response of canopy air warming to the addition of anthropogenic heat flux is mostly due to decreases in λ_2 (i.e., λ_2 becomes more negative) as ΔQ_{AH} increases (figure 5). For example, the differences between AH100 and AH1 in terms of λ_2 give median values of -13% and -28% in summer and winter, respectively. As alluded to earlier in Section 3.1, λ_2 is associated with changes in the atmosphere-canopy air heat conductance (Δc_a). These results imply that with a larger ΔQ_{AH}, the increase in c_a is stronger, leading to a more negative λ_2 and a weaker $\Delta T_a/\Delta Q_{AH}$. Therefore, the nonlinear response of ΔT_a to ΔQ_{AH} is traced to the role of c_a.

4. Discussion

There are several implications of this study that are important to appreciate. First, we argue that it is equally important to study the sensitivity ($\Delta T_a/\Delta Q_{AH}$) in addition to the forcing magnitude (ΔQ_{AH}). The sensitivity is the ratio of the response (ΔT_a) to the forcing and is a much better constrained quantity than the response itself, as can be seen from table 1. Second, the forcing-feedback framework further allows us to understand why many previous studies reported a sensitivity ($\Delta T_a/\Delta Q_{AH}$) of about 0.01 $K(W\ m^{-2})^{-1}$. Without considering any feedbacks and any role of c_s (both are reasonably good assumptions), the baseline sensitivity is $\lambda_o \approx 100$ W m^{-2} K^{-1} ($\rho \approx 1$ kg m^{-3}, $c_p \approx 1000$ J kg^{-1} K^{-1} and $c_a \approx 0.1$ m s^{-1}), yielding a sensitivity $\Delta T_a/\Delta Q_{AH}$ of 0.01 $K(W\ m^{-2})^{-1}$. Third, the forcing-feedback framework allows us to quantify the contributions of various physical processes to the spatiotemporal variability of $\Delta T_a/\Delta Q_{AH}$. Our results demonstrate that the atmosphere-canopy air heat conductance (c_a) plays a central role in controlling the spatiotemporal variations of $\Delta T_a/\Delta Q_{AH}$, as well as the nonlinear response of ΔT_a to ΔQ_{AH}. Hence, it is critical for urban canopy models to accurately represent the convective heat transfer between

379 the canopy air and the overlying atmosphere, among other things. Currently, Monin-Obukhov
380 similarity theory remains the workhorse model to parameterize c_a in urban canopy models due to
381 its popularity and parsimony (e.g., in CLMU see Oleson *et al* 2008a), even though urban areas are
382 not homogeneous and thus Monin-Obukhov similarity theory does not strictly apply (Garratt
383 1994). It remains unclear whether Monin-Obukhov similarity theory combined with urban
384 roughness lengths are sufficient for parameterizing c_a over urban areas or new theories accounting
385 for the effects of urban canopies (e.g., similar to the work by Harman and Finnigan (2007, 2008),
386 see also Bonan *et al* (2018)) are needed. Furthermore, in this context nearly all urban canopy
387 models assume that turbulent transport is the only process that needs to be parameterized.
388 However, dispersive transport might become relevant over areas with large variations of building
389 heights (Akinlabi *et al* 2022). Addressing these questions is outside the scope of this study but is
390 strongly needed.

391 There are also limitations of this work that need to be pointed out. First, we only evaluate the
392 feedback processes within the urban canopy layer. Quantifying the role of atmospheric feedback
393 (λ_4) and how it is scale-dependent (Li and Wang 2019) is left for future work. Second, while we
394 highlight the central role played by the atmosphere-canopy air heat conductance (c_a), diagnosing
395 the physical processes as well as urban morphological parameters that give rise to the
396 spatiotemporal variability of c_a (e.g., diagnosing the differences between different cities in figure
397 4) remains to be conducted. Within the confines of Monin-Obukhov similarity theory, c_a is
398 affected by shear-generated and buoyancy-generated turbulence and is a function of mean wind
399 speed, roughness lengths (both momentum and thermal roughness lengths), and stability
400 parameters. The momentum roughness length is further a complex function of building height and
401 canyon geometry. Understanding the spatiotemporal variability of c_a and its relation to these

underlying factors is beyond the scope of this study. Third, this study does not prescribe spatially and temporally varying anthropogenic heat flux. This is justified by the focus of this work on the sensitivity ($\Delta T_a/\Delta Q_{AH}$) instead of the response (ΔT_a). The temperature response (ΔT_a) can be viewed as the product of the sensitivity ($\Delta T_a/\Delta Q_{AH}$) and the forcing (ΔQ_{AH}). Thus, the spatiotemporal variability of temperature response is further complicated by the spatiotemporal variability of the forcing. Studies aiming to quantify the temperature response should also address the variability of the forcing.

5. Conclusion

Anthropogenic heat flux is an important control of the urban thermal environment. Although many studies investigated the impacts of anthropogenic heat flux, the key factors controlling the magnitude of the sensitivity of urban air temperature to anthropogenic heat flux ($\Delta T_a/\Delta Q_{AH}$) and its spatial and temporal patterns remain elusive. In this study, we develop a forcing-feedback framework based on the energy balance of air within the urban canopy layer and apply the framework to diagnosing simulated $\Delta T_a/\Delta Q_{AH}$ over CONUS by a numerical model. Within the forcing-feedback framework, the sensitivity ($\Delta T_a/\Delta Q_{AH}$) is decomposed into the direct effect of Q_{AH} on T_a, as well as feedbacks through changes in the surface temperature (T_s), the atmosphere-canopy air heat conductance (c_a), and the surface-canopy air heat conductance (c_s). This forcing-feedback framework allows us, for the first time, to understand the contributions of physical processes within the UCL to $\Delta T_a/\Delta Q_{AH}$ and the spatiotemporal variability of $\Delta T_a/\Delta Q_{AH}$ in a quantitative manner.

Our study first examines the seasonal variation of the sensitivity $\Delta T_a/\Delta Q_{AH}$. In summer, the positive feedback (mainly from changes in surface temperature, represented by λ_1) is nearly

cancelled by the negative feedback (mainly from changes in atmosphere-canopy air heat conductance c_a, represented by λ_2). As a result, the sensitivity $\Delta T_a/\Delta Q_{AH}$ is dominated by the direct effect (represented by λ_0). In winter, the negative feedback from c_a (represented by λ_2) weakens, leading to a stronger $\Delta T_a/\Delta Q_{AH}$. We also investigate the diurnal variations of $\Delta T_a/\Delta Q_{AH}$. The results show that the diurnal variations of $\Delta T_a/\Delta Q_{AH}$ are mostly controlled by the diurnal variations in λ_0, and to a less extent, λ_2, both of which are strongly related to the diurnal variations of c_a (and Δc_a). Hence, it can be summarized that the temporal (both seasonal and diurnal) dynamics of $\Delta T_a/\Delta Q_{AH}$ are mostly controlled by those of c_a. We also find that the spatial variability of $\Delta T_a/\Delta Q_{AH}$ over CONUS is mainly determined by the direct effect (λ_0). Since λ_0 is proportional to the sum of c_a and c_s, and c_s shows little spatial variability, the spatial variability of $\Delta T_a/\Delta Q_{AH}$ is dominated by the spatial variability of c_a. We further examine the nonlinearity in the response of ΔT_a to ΔQ_{AH} by varying the magnitude of ΔQ_{AH}. The nonlinear response of ΔT_a to ΔQ_{AH} stems mostly from the feedback process associated with changes in atmosphere-canopy air heat conductance (c_a). Our framework provides a tool to study the feedback mechanisms that are important for understanding the sensitivity of urban canopy air temperature to anthropogenic heat flux.

Acknowledgments

LW and DL acknowledge the financial support by the U.S. Department of Energy, Office of Science, as part of research in Multi-Sector Dynamics, Earth and Environmental System Modelling Program. The computing and data storage resources were provided by the National Energy Research Scientific Computing Center (NERSC), which is supported by the Office of Science of the U.S. Department under Contract No. DE-AC02-05Ch11231. DL also

446 acknowledges support from the U.S. National Science Foundation (Grant ICER-1854706). WZ is
447 supported by the U.S. DOE Office of Science Biological and Environmental Research as part of
448 the Regional and Global Modeling and Analysis program. The authors are grateful to Dr. Keith
449 Oleson at NCAR for insightful discussions. The CESM2 release code (release-cesm2.0.1) and
450 input data are available at
451 https://escomp.github.io/CESM/versions/cesm2.1/html/downloading_cesm.html.

452 Data availability statement

453 The data that support the findings of this study are openly available at the following URL/DOI:
454 https://doi.org/10.57931/1890465.

455 References

456 Akinlabi E, Maronga B, Giometto M G and Li D 2022 Dispersive fluxes within and over a real
457 urban canopy: A large-eddy simulation study *Bound.-Layer Meteorol.* **185** 93-128

458 Allen L, Lindberg F and Grimmond C S B 2011 Global to city scale urban anthropogenic heat
459 flux: Model and variability *Int. J. Climatol.* **31** 1990-2005

460 Block A, Keuler K and Schaller E 2004 Impacts of anthropogenic heat on regional climate
461 patterns *Geophys. Res. Lett.* **31** L12211

462 Bohnenstengel S I, Hamilton I, Davies M and Belcher S E 2014 Impact of anthropogenic heat
463 emissions on London's temperatures *Q. J. R. Meteorol. Soc.* **140** 687-698

464 Bonan G B, Patton E G, Harman I N, Oleson K W, Finnigan J J, Lu Y and Burakowski E A 2018
465 Modeling canopy-induced turbulence in the Earth system: a unified parameterization of

turbulent exchange within plant canopies and the roughness sublayer (CLM-ml v0) *Geosci. Model Dev.* **11** 1467-1496

Chan E Y Y, Goggins W B, Kim J J and Griffiths S M 2012 A study of intracity variation of temperature-related mortality and socioeconomic status among the Chinese population in Hong Kong *J. Epidemiol. Community Health* **66** 322

Chen Y, Jiang W M, Zhang N, He X F and Zhou R W 2009 Numerical simulation of the anthropogenic heat effect on urban boundary layer structure *Theor. Appl. Climatol.* **97** 123-134

Chow W T L, Salamanca F, Georgescu M, Mahalov A, Milne J M and Ruddell B L 2014 A multi-method and multi-scale approach for estimating city-wide anthropogenic heat fluxes *Atmos. Environ.* **99** 64-76

Danabasoglu G *et al* 2020 The Community Earth System Model Version 2 (CESM2) *J. Adv. Model. Earth Syst.* **12** e2019MS001916

Demuzere M, Oleson K, Coutts A M, Pigeon G and van Lipzig N P M 2013 Simulating the surface energy balance over two contrasting urban environments using the Community Land Model Urban *Int. J. Climatol.* **33** 3182-3205

Doan V Q, Kusaka H and Nguyen T M 2019 Roles of past, present, and future land use and anthropogenic heat release changes on urban heat island effects in Hanoi, Vietnam: Numerical experiments with a regional climate model *Sustain. Cities Soc.* **47** 101479

Fan H and Sailor D J 2005 Modeling the impacts of anthropogenic heating on the urban climate of Philadelphia: a comparison of implementations in two PBL schemes *Atmos. Environ.* **39** 73-84

Feng J, Wang Y, Ma Z and Liu Y 2012 Simulating the regional impacts of urbanization and anthropogenic heat release on climate across China *J. Climate* **25** 7187-7203

Feng J, Wang J and Yan Z 2014 Impact of anthropogenic heat release on regional climate in three vast urban agglomerations in China *Adv. Atmos. Sci.* **31** 363-373

Fink G, Schmid M and Wüest A 2014 Large lakes as sources and sinks of anthropogenic heat: Capacities and limits *Water Resour. Res.* **50** 7285-7301

Flanner M G 2009 Integrating anthropogenic heat flux with global climate models *Geophys. Res. Lett.* **36**

Garratt J R, 1994: *The Atmospheric Boundary Layer.* Cambridge University Press, 316 pp.

Grimmond C S B *et al* 2011 Initial results from Phase 2 of the international urban energy balance model comparison *Int. J. Climatol.* **31** 244-272

Harman I N and Finnigan J J 2007 A simple unified theory for flow in the canopy and roughness sublayer *Bound.-Layer Meteorol.* **123** 339-363

Harman I N and Finnigan J J 2008 Scalar concentration profiles in the canopy and roughness sublayer *Bound.-Layer Meteorol.* **129** 323-351

Ichinose T, Shimodozono K and Hanaki K 1999 Impact of anthropogenic heat on urban climate in Tokyo *Atmos. Environ.* **33** 3897-3909

Jackson T L, Feddema J J, Oleson K W, Bonan G B and Bauer J T 2010 Parameterization of urban characteristics for global climate modeling *Ann. Assoc. Am. Geogr.* **100** 848-865

Jin K, Wang F and Wang S 2020 Assessing the spatiotemporal variation in anthropogenic heat and its impact on the surface thermal environment over global land areas *Sustain. Cities Soc.* **63** 102488

Karsisto P *et al* 2016 Seasonal surface urban energy balance and wintertime stability simulated using three land-surface models in the high-latitude city Helsinki *Q. J. R. Meteorol. Soc.* **142** 401-417

Kikegawa Y, Tanaka A, Ohashi Y, Ihara T and Shigeta Y 2014 Observed and simulated sensitivities of summertime urban surface air temperatures to anthropogenic heat in downtown areas of two Japanese Major Cities, Tokyo and Osaka *Theor. Appl. Climatol.* **117** 175-193

Krpo A, Salamanca F, Martilli A and Clappier A 2010 On the impact of anthropogenic heat fluxes on the urban boundary layer: A two-dimensional numerical study *Bound.-Layer Meteorol.* **136** 105-127

Li D and Wang L 2019 Sensitivity of surface temperature to land use and land cover change-induced biophysical changes: The scale issue *Geophys. Res. Lett.* **46** 9678-9689

Liu S *et al* 2020 Global river water warming due to climate change and anthropogenic heat emission *Glob. Planet. Change* **193** 103289

Ma S, Pitman A, Hart M, Evans J P, Haghdadi N and MacGill I 2017 The impact of an urban canopy and anthropogenic heat fluxes on Sydney's climate *Int. J. Climatol.* **37** 255-270

Mei S-J and Yuan C 2021 Analytical and numerical study on transient urban street air warming induced by anthropogenic heat emission *Energy Build.* **231** 110613

528 Molnár G, Kovács A and Gál T 2020 How does anthropogenic heating affect the thermal
529 environment in a medium-sized Central European city? A case study in Szeged, Hungary
530 *Urban Clim.* **34** 100673

531 Mora C *et al* 2017 Global risk of deadly heat *Nat. Clim. Change* **7** 501-506

532 Narumi D, Kondo A and Shimoda Y 2009 Effects of anthropogenic heat release upon the urban
533 climate in a Japanese megacity *Environ. Res.* **109** 421-431

534 United Nations, 2022: Goal 11: Make cities inclusive, safe, resilient and sustainable (Available
535 at: https://www.un.org/sustainabledevelopment/cities/) (accessed 28 September 2022)

536 Oleson K W, Bonan G B, Feddema J, Vertenstein M and Grimmond C S B 2008a An urban
537 parameterization for a global climate model. Part I: Formulation and evaluation for two
538 cities *J. Appl. Meteor. Climatol.* **47** 1038-1060

539 Oleson K W, Bonan G B, Feddema J and Vertenstein M 2008b An urban parameterization for a
540 global climate model. Part II: Sensitivity to input parameters and the simulated urban heat
541 island in offline Simulations *J. Appl. Meteor. Climatol.* **47** 1061-1076

542 Oleson K W, Bonan G B, Feddema J, Vertenstein M and Kluzek E 2010 Technical description of
543 an urban parameterization for the Community Land Model (CLMU) (No. NCAR/TN-
544 480+STR) Technical Report, UCAR/NCAR https://doi.org/10.5065/D6K35RM9

545 Oleson K W, Bonan G B, Feddema J and Jackson T 2011 An examination of urban heat island
546 characteristics in a global climate model *Int. J. Climatol.* **31** 1848-1865

547 Oleson K W and Feddema J 2020 Parameterization and surface data improvements and new
548 capabilities for the Community Land Model Urban (CLMU) *J. Adv. Model. Earth Syst.* **12**
549 e2018MS001586

Sailor D J and Lu L 2004 A top–down methodology for developing diurnal and seasonal anthropogenic heating profiles for urban areas *Atmos. Environ.* **38** 2737-2748

Sailor D J 2011 A review of methods for estimating anthropogenic heat and moisture emissions in the urban environment *Int. J. Climatol.* **31** 189-199

Sailor D J, Georgescu M, Milne J M and Hart M A 2015 Development of a national anthropogenic heating database with an extrapolation for international cities *Atmos. Environ.* **118** 7-18

Salamanca F, Georgescu M, Mahalov A, Moustaoui M and Wang M 2014 Anthropogenic heating of the urban environment due to air conditioning *J. Geophys. Res. Atmos.* **119** 5949-5965

Suga M, Almkvist E, Oda R, Kusaka H and Kanda M 2009 The impacts of anthropogenic energy and urban canopy model on urban atmosphere *Annu. J. Hydraul. Eng.* **53** 283-288

Sun R, Wang Y and Chen L 2018 A distributed model for quantifying temporal-spatial patterns of anthropogenic heat based on energy consumption *J. Cleaner Prod.* **170** 601-609

Wang L, Huang M and Li D 2020 Where Are White Roofs More Effective in Cooling the Surface? *Geophys. Res. Lett.* **47** e2020GL087853

Wang L, Huang M and Li D 2021 Strong influence of convective heat transfer efficiency on the cooling benefits of green roof irrigation *Environ. Res. Lett.* **16** 084062

Xia Y *et al* 2012 Continental-scale water and energy flux analysis and validation for the North American Land Data Assimilation System project phase 2 (NLDAS-2): 1. Intercomparison and application of model products *J. Geophys. Res. Atmos.* **117** D03109

571 Xie M *et al* 2016 Changes in regional meteorology induced by anthropogenic heat and their
572 impacts on air quality in South China *Atmos. Chem. Phys.* **16** 15011-15031

573 Yang W, Luan Y, Liu X, Yu X, Miao L and Cui X 2017 A new global anthropogenic heat
574 estimation based on high-resolution nighttime light data *Sci. Data* **4** 170116

575 Zhang N, Wang X, Chen Y, Dai W and Wang X 2016 Numerical simulations on influence of
576 urban land cover expansion and anthropogenic heat release on urban meteorological
577 environment in Pearl River Delta *Theor. Appl. Climatol.* **126** 469-479
578

579 **Table 1.** A selected list of existing studies on the warming effect of anthropogenic heat emissions.
580 Note that most values for $\Delta T_a/\Delta Q_{AH}$ are rough estimates based on the data in these studies, except
581 the work of Kikegawa *et al* (2014).

Reference	Region	Model	Peak AH ($W\ m^{-2}$)	Peak ΔT_a (K)	Estimated $\frac{\Delta T_a}{\Delta Q_{AH}}$ ($K\ (W\ m^{-2})^{-1}$)
Ichinose *et al* (1999)	Tokyo, Japan	The Colorado State University Mesoscale Model (CSU-MM)	1590	2.5	0.001 - 0.05
Fan; Sailor (2005)	Philadelphia, USA	MM5	90	3	0.003 - 0.03
Narumi *et al* (2009)	Keihanshin, Japan	Model in Pielke (1974)	115	0.6	0.005 - 0.01
Feng *et al* (2012)	China	WRF	50	0.15	0.003
de Munck *et al* (2013)	Paris, France	A coupled model consisting of the non-hydrostatic meso-scale atmospheric model (MESO-NH)	34	0.5	0.015
Bohnenstengel *et al* (2014)	London, UK	The Met Office-Reading Urban Surface Exchange Scheme (MORUSES)	400	3	0.008
Kikegawa et *al* (2014)	Tokyo and Osaka, Japan	Observations and WRF-CM-BEM	220	-	0.005 - 0.012
Feng *et al* (2014)	East China	WRF	45	0.9	0.02
Wang *et al* (2015)	Yangtze River Delta	WRF	50	0.9	0.018
Zhang *et al* (2016)	Pearl River Delta, China	WRF	405	3.37	0.008
Ma *et al* (2017)	Sydney, Australia	WRF	60	1.5	0.025
Doan *et al* (2019)	Hanoi, Vietnam	WRF	100	0.7	0.007

Yang *et al* (2019)	Yangtze River Delta, China	WRF	150	1	0.007
Molnár *et al* (2020)	Szeged, Hungary	WRF	31	1.5	0.05
Mei; Yuan (2021)	Newton, Singapore	An analytical model and Large-Eddy Simulation (LES)	15	0.45	0.03

582

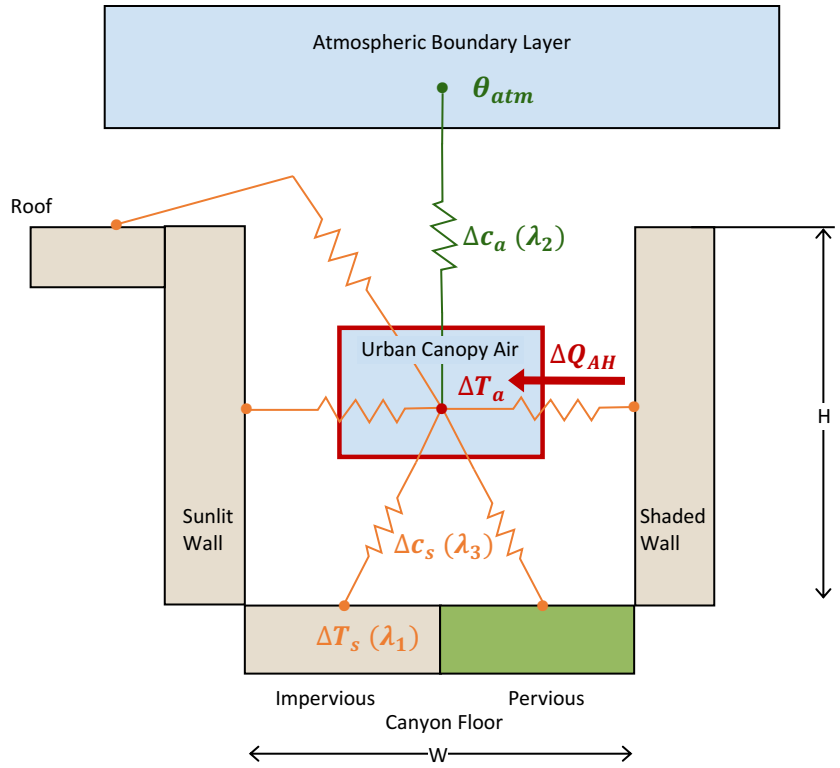

583

584 **Figure 1.** Schematic of the forcing-feedback framework for understanding the impact of
585 anthropogenic heat flux (ΔQ_{AH}) on canopy air temperature (T_a). In this framework, the
586 anthropogenic heat flux perturbs the energy budget of the canopy air, directly altering T_a and
587 further influencing the changes in surface temperatures (T_s) of multiple urban facets, the heat
588 conductance between the canopy air and urban surfaces (c_s), and the heat conductance between
589 the canopy air and overlying atmosphere (c_a). Besides the direct effect of Q_{AH} on T_a, there also
590 exists important feedbacks: λ_1 refers to the strength of feedback from ΔT_s; λ_2 is the feedback
591 parameter for Δc_a; λ_3 is the feedback parameter for Δc_s. *Source*: adapted from Oleson *et al.*
592 (2010).

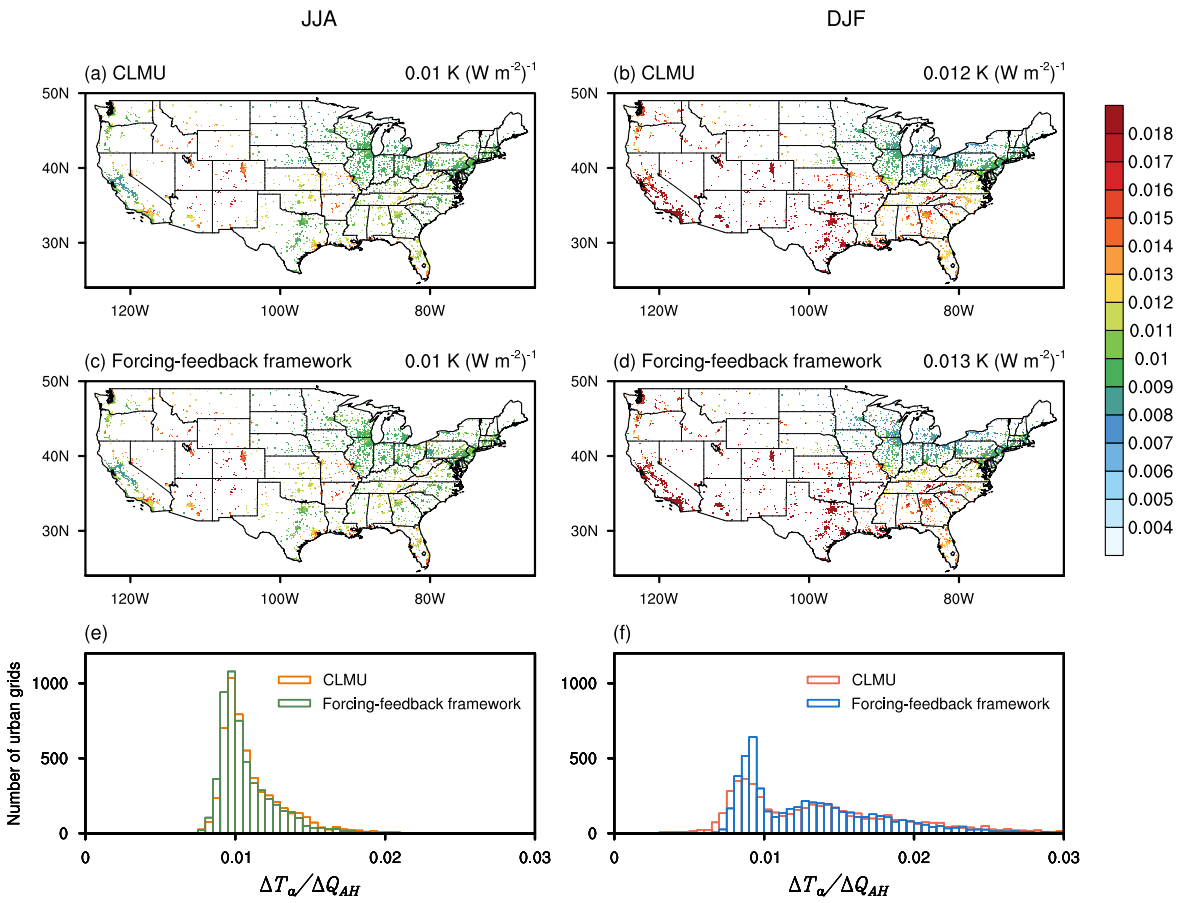

593

594 **Figure 2.** The sensitivity of canopy air temperature to anthropogenic heat flux $\Delta T_a/\Delta Q_{AH}$
595 simulated by CLMU and diagnosed from the proposed forcing-feedback framework. (a), (c), (e)
596 are for JJA, (b), (d), (f) are for DJF, and (e), (f) are histograms for the sensitivity $\Delta T_a/\Delta Q_{AH}$. The
597 median value over CONUS is also shown at the top right of each map. All units are $K\ (W\ m^{-2})^{-1}$.
598 The results are from AH1. Only grid cells with more than 0.1% of urban land are shown and
599 analyzed.

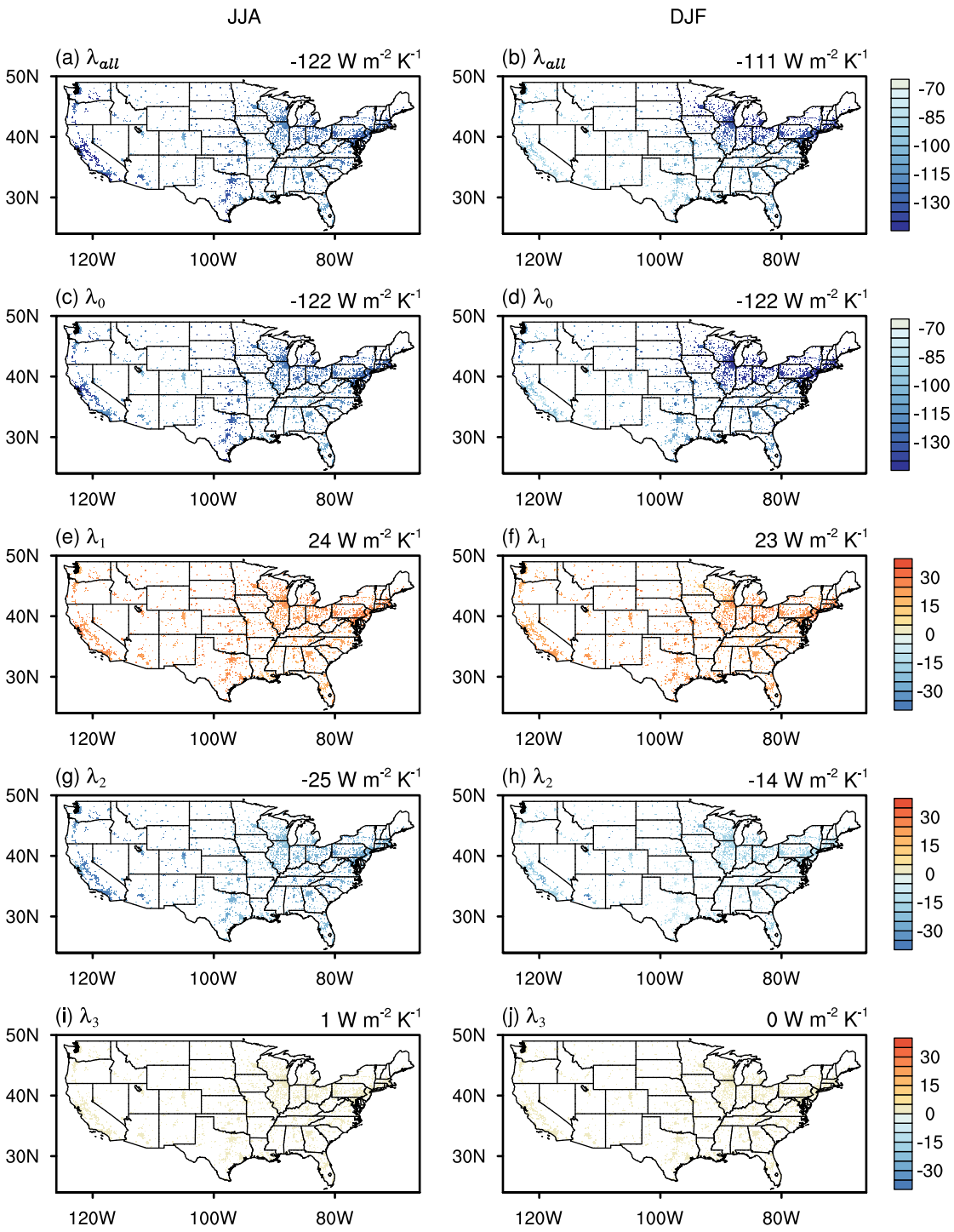

600

601 **Figure 3.** The sensitivity and feedback parameters: (a-b) the total sensitivity parameter (λ_{all}), (c-
602 d) the baseline sensitivity parameter (λ_o), and the feedback parameter for the (e-f) surface
603 temperature (λ_1), (g-h) heat conductance between the canopy air and overlying atmosphere (λ_2),

(i-j) heat conductance between the canopy air and urban surfaces (λ_3). (a), (c), (e), (g), (i) are for JJA, (b), (d), (f), (h), (j) are for DJF. The median value over CONUS is also shown at the top right of each map. All units are $W\ m^{-2}\ K^{-1}$. The results are from AH1. Only grid cells with more than 0.1% of urban land are shown.

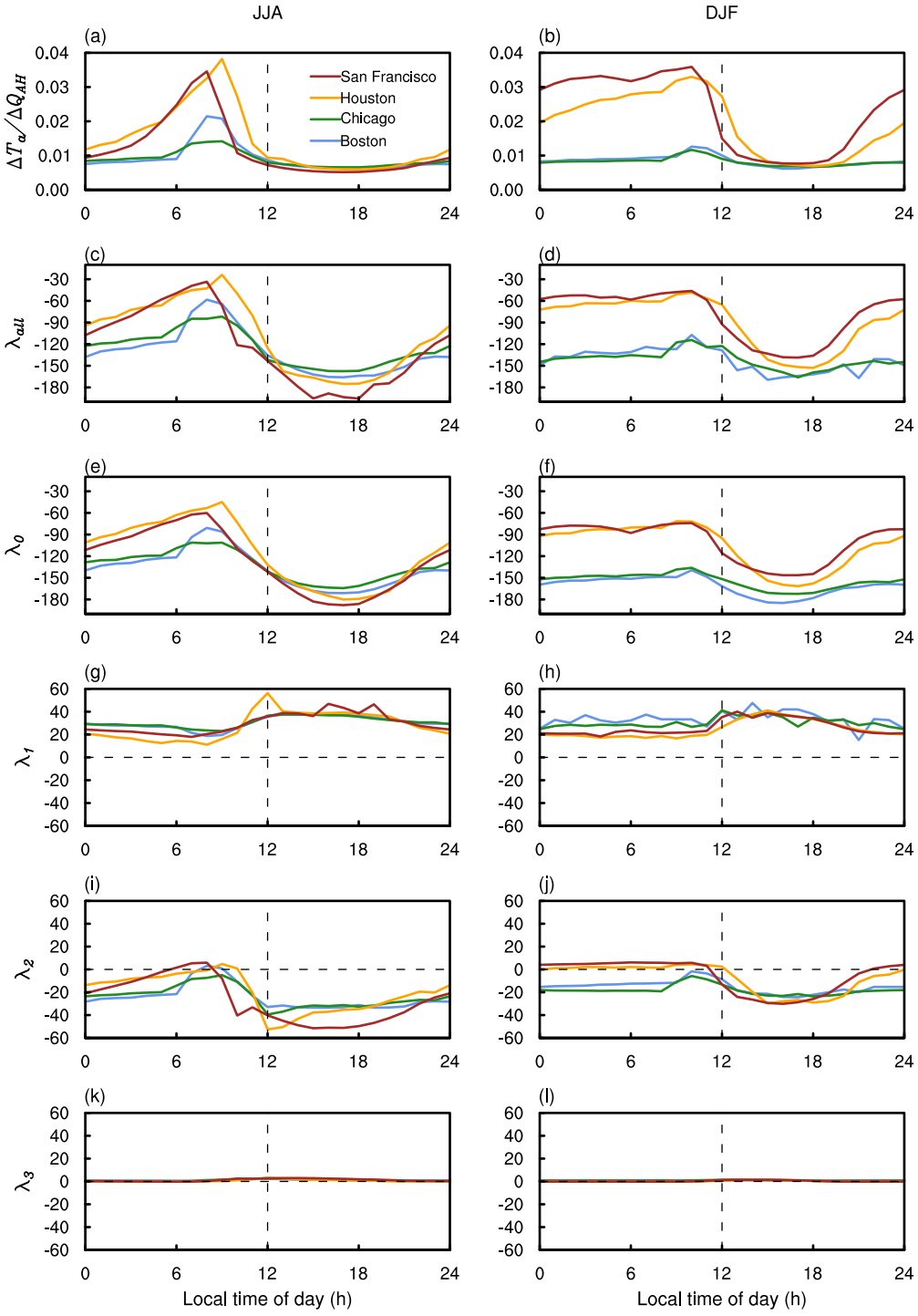

609

610 **Figure 4.** Diurnal cycles of (a-b) the sensitivity $\Delta T_a/\Delta Q_{AH}$ (unit: $K\ (W\ m^{-2})^{-1}$), and feedback

611 parameters (c-d) λ_{all}, (e-f) λ_0, (g-h) λ_1, (i-j) λ_2, (k-l) λ_3 (unit: $W\ m^{-2}\ K^{-1}$) in four cities (San

612 Francisco, Boston, Chicago, and Houston). (a), (c), (e), (g), (i), (k) are for JJA, (b), (d), (f), (h), (j),

613 (l) are for DJF.

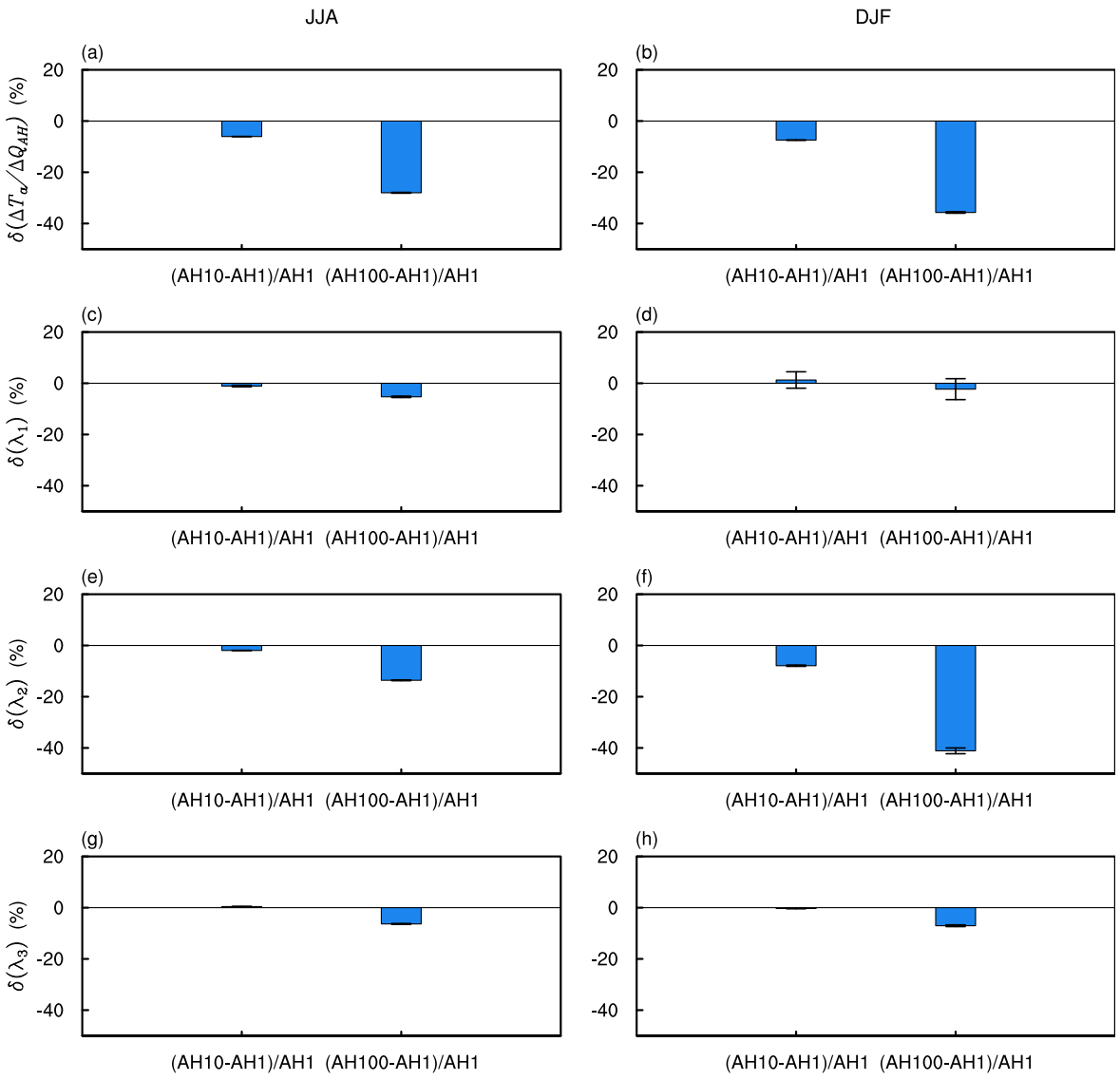

614

615 **Figure 5.** Relative changes (represented by δ, %) in (a-b) the sensitivity $\Delta T_a/\Delta Q_{AH}$, and feedback
616 parameters (c-d) λ_1, (e-f) λ_2, (g-h) λ_3 by comparing AH10 and AH100 to AH1 (i.e., the results of
617 AH10 and AH100 minus the results of AH1 and then normalized by the results of AH1). The error
618 bars show 95% confidence interval over CONUS. (a), (c), (e), (g) are for JJA, (b), (d), (f), (h) are
619 for DJF.